

Model of Vortex Turbulent Plane Couette Flow

Victor L. Mironov and Sergey V. Mironov

Institute for physics of microstructures RAS, Nizhny Novgorod, Russia;

e-mail: mironov@ipmras.ru

Abstract. We present the theoretical studies of plane Couette flow between two moving plates based on the previously proposed equations of vortex fluid, which take into account both the longitudinal flow and the vortex tubes rotation. It is shown that there are several stationary solutions. One of them describes a laminar flow strongly localized in the regions near the plate surfaces. The classical linear distribution of the flow velocity corresponds to in-phase tubes rotation. We also discuss the model of flow with different phases of tubes rotation, which is applied to the description of the turbulent Couette flow. In particular, it is shown that, in the simple Boussinesq approximation, the calculated stationary profiles of mean velocity in turbulent flow coincide with experimental data and results of direct numerical simulations.

Keywords: viscous fluid; vortex plane Couette flow; turbulent flow; Boussinesq approximation

1. Introduction

To describe vortex flows, many authors construct Maxwell-type symmetric equations for the local velocity and vorticity vectors [1–6]. In particular, these equations are used for the description of turbulent flows [4] and electron-ion plasma in the framework of a hydrodynamic two-fluid model [7–10]. However, in all mentioned papers, the additional equation for vortex motion is obtained by taking the "curl" operator from the Euler equation and hence the resulting equation is not independent. Recently, we have developed an alternative approach based on the droplet model of a liquid introduced by Helmholtz [11] and have obtained a closed system of Maxwell-type equations for vortex flow, taking into account the rotation and twisting of vortex tubes [12]. In particular, we applied this approach to derive self-consistent hydrodynamic equations for electron-ion plasma [13] and electron fluids in solids [14].

In the present paper, we apply proposed equations to describe the plane Couette flow between two moving plates [15,16]. This is a relatively simple type of shear flow, which is actively studied both theoretically and experimentally. At present, extensive experimental material has been accumulated on studies of laminar and turbulent Couette flow [17-21]. Theoretical consideration of the Couette flow is carried out using semi-empirical analytical models [22-24] and direct numerical simulations (DNS) [25-28] based on the solution of the Navier-Stocks equation. The system of vortex fluid equations [12] includes an additional equation for vortex tube rotation that allows us to construct a simple analytical model of the turbulent Couette flow, which adequately describes the mean velocity profiles for different Reynolds numbers (Re).

2. Equations for vortex flow of viscous fluid

As we showed in [12], a vortex isentropic flow of viscous fluid is described by the following symmetric system of equations:

$$\begin{aligned} \frac{1}{c} \left(\frac{\partial}{\partial t} + (\vec{v} \cdot \vec{\nabla}) - \mu \Delta \right) \vec{v} + \vec{\nabla} \times \vec{w} + \vec{\nabla} u &= 0, \\ \frac{1}{c} \left(\frac{\partial}{\partial t} + (\vec{v} \cdot \vec{\nabla}) - \mu \Delta \right) u + \vec{\nabla} \cdot \vec{v} &= 0, \\ \frac{1}{c} \left(\frac{\partial}{\partial t} + (\vec{v} \cdot \vec{\nabla}) - \mu \Delta \right) \vec{w} - \vec{\nabla} \times \vec{v} + \vec{\nabla} \xi &= 0, \\ \frac{1}{c} \left(\frac{\partial}{\partial t} + (\vec{v} \cdot \vec{\nabla}) - \mu \Delta \right) \xi + \vec{\nabla} \cdot \vec{w} &= 0. \end{aligned} \tag{1}$$

Here c is a speed of sound, \vec{v} is a local velocity, μ is the coefficient of kinematic viscosity, $\vec{\nabla}$ is the Hamilton operator, Δ is the Laplace operator. The value u is proportional to the enthalpy

$$\begin{aligned} u &= \frac{1}{c} \varepsilon, \\ d\varepsilon &= \frac{c^2}{\rho} d\rho, \end{aligned} \quad (2)$$

where ε is an enthalpy per unit mass, ρ is a fluid density. The vector \vec{w} characterizes the rotation of the vortex tube around its axis

$$\begin{aligned} \vec{w} &= 2c\vec{\theta}, \\ \vec{\omega} &= \frac{d\vec{\theta}}{dt}, \end{aligned} \quad (3)$$

where $\vec{\theta}$ is the angular vector of rotation of the vortex tube, $\vec{\omega}$ is the angular velocity of the vortex tube rotation. The value ξ characterizes the twisting of the vortex tube

$$|\xi| = c\gamma, \quad (4)$$

where γ is the twisting angle of the vortex tube [12].

Further we will use a simplified model to describe the flow of viscous vortex fluid. We assume that the liquid is incompressible ($\rho = \text{const}$, $u = \text{const}$) and neglect the twisting of the vortex tubes ($\xi = 0$). Then the system of equations describing the motion of the fluid takes the following form:

$$\begin{aligned} \frac{1}{c} \left(\frac{\partial}{\partial t} + (\vec{v} \cdot \vec{\nabla}) - \mu \Delta \right) \vec{v} + \vec{\nabla} \times \vec{w} &= 0, \\ \frac{1}{c} \left(\frac{\partial}{\partial t} + (\vec{v} \cdot \vec{\nabla}) - \mu \Delta \right) \vec{w} - \vec{\nabla} \times \vec{v} &= 0, \\ \vec{\nabla} \cdot \vec{v} &= 0, \\ \vec{\nabla} \cdot \vec{w} &= 0. \end{aligned} \quad (5)$$

These equations make it possible to take into account the effects associated with the rotation of vortex tubes during fluid motion.

3. Plane flow between two moving plates

Let us consider a stationary flow of viscous fluid formed between two infinite, parallel plates moving relative to each other (Figure 1). We denote the speed of the plates as v and assume that all quantities in a steady flow depend only on the transverse coordinate y .

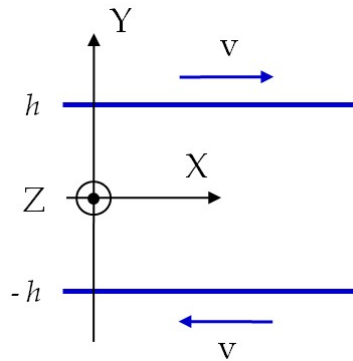


Figure 1. Sketch of a system consisting of fluid placed between two infinite plates, which move along the X axis with speed v in opposite directions.

In the next sections we consider various types of possible flows in this channel, which are described by the system of equations (5).

4. Laminar flow without rotation of vortex tubes

First, we consider a stationary flow, when the angular velocity of the vortex tubes rotation is equal to zero ($\vec{\omega} = 0$). We assume that the functions $\vec{v}(y)$ and $\vec{w}(y)$ are time-independent. Then the system of equations (5) takes the following form:

$$\begin{aligned} \frac{1}{c}(\vec{v} \cdot \vec{\nabla} - \mu \Delta) \vec{v} + \vec{\nabla} \times \vec{w} &= 0, \\ \frac{1}{c}(\vec{v} \cdot \vec{\nabla} - \mu \Delta) \vec{w} - \vec{\nabla} \times \vec{v} &= 0, \\ \vec{\nabla} \cdot \vec{v} &= 0, \\ \vec{\nabla} \cdot \vec{w} &= 0. \end{aligned} \quad (6)$$

For one-dimensional motion along the X axis, only the x-component of $\vec{v}(y)$ is nonzero, which we denote as v_x . Accordingly, only the z-component of the vector $\vec{w}(y)$ is nonzero, which we denote as w_z ($w_z = 2c\theta_z$). Projecting the first equation of system (6) onto the X axis, and the second equation onto the Z axis, we obtain the following system:

$$\begin{aligned} -\lambda \frac{\partial^2 v_x}{\partial y^2} + \frac{\partial w_z}{\partial y} &= 0, \\ -\lambda \frac{\partial^2 w_z}{\partial y^2} + \frac{\partial v_x}{\partial y} &= 0. \end{aligned} \quad (7)$$

Here the parameter $\lambda = \mu/c$. In addition, we assume that for the liquid at the plate surfaces the conditions of complete no-slip are realized. This brings us to the following boundary conditions

$$\begin{aligned} v_x(h) &= v, \\ v_x(-h) &= -v, \\ \theta_z(h) &= \theta_z(-h) = 0. \end{aligned} \quad (8)$$

The solutions of system (7) satisfying the boundary conditions (8) are

$$v_x = v \frac{\sinh(y/\lambda)}{\sinh(h/\lambda)}, \quad (9)$$

$$\theta_z = \frac{v}{2c} \frac{\cosh(y/\lambda) - \cosh(h/\lambda)}{\sinh(h/\lambda)}. \quad (10)$$

The velocity distribution in the channel between the plates is shown schematically in Figure 2.

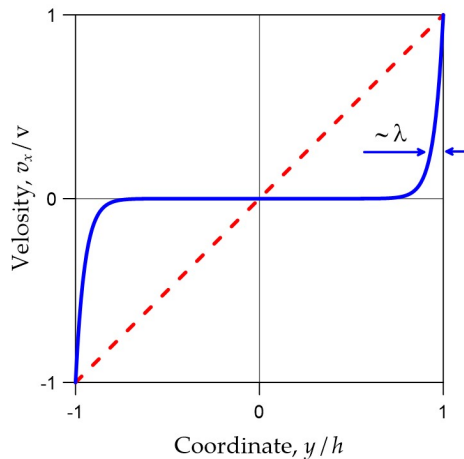


Figure 2. The distributions of steady velocity of the fluid between two moving plates. The solid blue line corresponds to distribution (9). The dotted red line corresponds to distribution (15).

Since for the majority of experimentally realized channels (except very thin capillary channels) $h/\lambda \gg 1$, then such laminar flow is realized only near the plates surface.

Schematically, the distribution of the angle of the vortex tubes rotation (10) is shown in Figure 3.

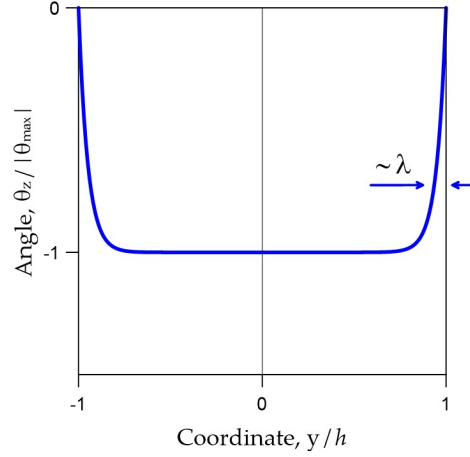


Figure 3. Schematic normalized distribution of the angle of the vortex tubes rotation (10) across the channel.

According to (9) the vortex of velocity (vorticity, $\vec{\Omega} = \vec{\nabla} \times \vec{v}$) has only z-component, which is equal to

$$\Omega_z = -\frac{v \cosh(y/\lambda)}{\lambda \sinh(h/\lambda)}. \quad (11)$$

The distribution of the vorticity in the channel between the plates is shown schematically in Figure 4.

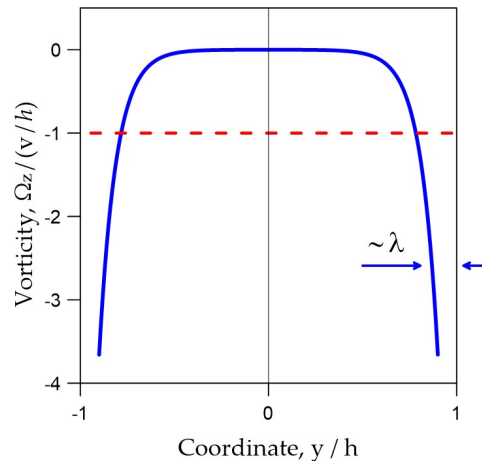


Figure 4. Distributions of vorticity in the channel between two moving plates. The solid blue line corresponds to distribution (11). The dotted red line corresponds to distribution (18).

5. Flow with in-phase rotation of vortex tubes

Another stationary flow satisfying Equations (5) is characterized by a field of vortex tubes uniformly rotating at constant angular velocity $\omega_z = const$ and having equal phases. We find a solution for the angle of vortex tubes rotation as

$$w_z(t) = 2c\omega_z t. \quad (12)$$

In this case the system (5) projected on the X and Z axes takes the following form:

$$\begin{aligned}\frac{\partial^2 v_x}{\partial y^2} &= 0, \\ 2\omega_z + \frac{\partial v_x}{\partial y} &= 0,\end{aligned}\tag{13}$$

with boundary conditions

$$\begin{aligned}v_x(h) &= v, \\ v_x(-h) &= -v, \\ \theta_z(h) &= \theta_z(-h) = \omega_z t.\end{aligned}\tag{14}$$

From the first equation of system (13) we obtain

$$v_x = \frac{v}{h} y.\tag{15}$$

From the expression (12) we have

$$\theta_z(t) = \omega_z t.\tag{16}$$

From the second equation of system (13) we obtain the relationship between the angular velocity of tubes rotation and the velocity of the plates

$$\omega_z = -\frac{v}{2h}.\tag{17}$$

Expression (17) shows that in this case the vortex tubes rotate with the maximum angular velocity determined by the speed of the plates. The vorticity is constant over the channel cross section and is equal to

$$\Omega_z = -\frac{v}{h} = 2\omega_z.\tag{18}$$

The distribution of velocity (15) and vorticity (18) are shown in Figures 2 and 4 by dotted lines. Stationary distributions (15) and (18) coincide with the known classical solutions for the Couette flow.

6. Rotation of vortex tubes with different phases

Let us consider a stationary flow consisting of vortex tubes oriented along the Z axis and uniformly rotating with a constant angular velocity $\omega_z = const$, but with different phases $\varphi_z(y)$ depending on the y coordinate. We will look for a solution in the form

$$w_z(y, t) = 2c\omega_z t + \varphi_z(y).\tag{19}$$

In this case, the first two equations of the system (5) in projections on the X and Z axes take the form

$$\begin{aligned}-\lambda \frac{\partial^2 v_x}{\partial y^2} + \frac{\partial \varphi_z}{\partial y} &= 0, \\ -\lambda \frac{\partial^2 \varphi_z}{\partial y^2} + \frac{\partial v_x}{\partial y} + 2\omega_z &= 0.\end{aligned}\tag{20}$$

We take the following boundary conditions:

$$\begin{aligned}v_x(h) &= v, \\ v_x(-h) &= -v, \\ \theta_z(h) &= \theta_z(-h) = \omega_z t.\end{aligned}\tag{21}$$

The solution of system (20) can be represented in the following form:

$$v_x = \alpha v \frac{y}{h} + (1-\alpha)v \frac{\sinh(y/\lambda)}{\sinh(h/\lambda)}, \quad (22)$$

$$\theta_z = -\alpha \frac{v}{2h} t + (1-\alpha) \frac{v}{2c} \frac{\cosh(y/\lambda) - \cosh(h/\lambda)}{\sinh(h/\lambda)}, \quad (23)$$

where dimensionless parameter α is

$$\alpha = \frac{2\omega_z h}{v}. \quad (24)$$

Schematic distribution of mean-velocity over the channel cross section is shown in Figure 5. Note that in the case of $\alpha=0$ the solutions (22)-(24) are reduced to (9)-(10), and in the case of $\alpha=1$ these solutions are reduced to (15)-(17).

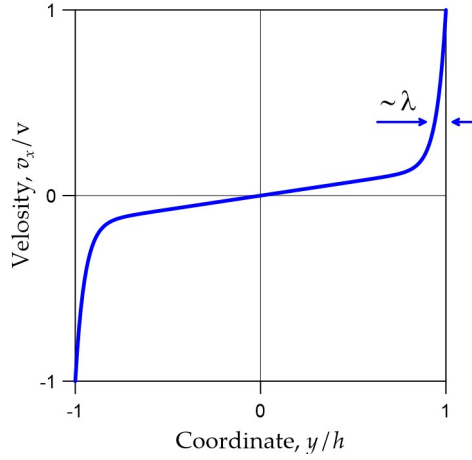


Figure 5. Distribution (22) corresponding to the fluid velocity in the channel between two moving plates.

7. Turbulent Couette flow

To describe a turbulent flow, we introduce the time-averaged values of the flow velocities in the xy plane, denoting them as \bar{v}_x, \bar{v}_y and corresponding fluctuations v'_x, v'_y . Then the local velocities of the turbulent flow are written in the following form:

$$\begin{aligned} v_x &= \bar{v}_x + v'_x, \\ v_y &= \bar{v}_y + v'_y, \\ v_z &= \bar{v}_z + v'_z. \end{aligned} \quad (25)$$

Similarly, for the vector of rotation \bar{w} we have

$$\begin{aligned} w_x &= \bar{w}_x + w'_x, \\ w_y &= \bar{w}_y + w'_y, \\ w_z &= \bar{w}_z + w'_z. \end{aligned} \quad (26)$$

Let us consider a turbulent flow along the X axis. We take into account that mean velocity $\bar{v}_x(y)$ depends only on y . Also we assume that vortex tubes oriented along the Z axis and uniformly rotate with a constant angular velocity $\omega_z = const$, but with different phases $\bar{\varphi}_z(y)$. So, we will look for a solution in the form

$$\bar{w}_z(y, t) = 2c\omega_z t + \bar{\varphi}_z(y). \quad (27)$$

Substituting (25)-(27) into Equation (5), we will account that $\bar{v}_y = 0$ and fluctuations v'_x, v'_y depend only on y coordinate. Then averaging over time and considering projections on the X and Z axes we obtain:

$$\begin{aligned}
-\frac{\mu}{c} \frac{\partial^2 \bar{v}_x}{\partial y^2} + \frac{1}{c} \frac{\partial}{\partial y} \overline{v'_x v'_y} + \frac{\partial \bar{w}_z}{\partial y} &= 0, \\
\frac{1}{c} \frac{\partial \bar{w}_z}{\partial t} - \frac{\mu}{c} \frac{\partial^2 \bar{w}_z}{\partial y^2} + \frac{1}{c} \frac{\partial}{\partial y} \overline{w'_z w'_y} + \frac{\partial \bar{v}_x}{\partial y} &= 0.
\end{aligned} \tag{28}$$

Here $\overline{v'_x v'_y}$ and $\overline{w'_z w'_y}$ are the components of the corresponding Reynolds tensors [22, 29]. In the framework of Boussinesq approximation [30, 31], we have

$$-\overline{v'_x v'_y} = \mu_T \frac{\partial \bar{v}_x}{\partial y}, \tag{29}$$

$$-\overline{w'_z w'_y} = \mu_T \frac{\partial \bar{w}_z}{\partial y}, \tag{30}$$

where μ_T is the turbulent kinematic viscosity. Let us assume $\mu_T = const$, then the Equations (28) take the form

$$\begin{aligned}
-\frac{\mu + \mu_T}{c} \frac{\partial^2 \bar{v}_x}{\partial y^2} + \frac{\partial \bar{w}_z}{\partial y} &= 0, \\
\frac{1}{c} \frac{\partial \bar{w}_z}{\partial t} - \frac{\mu + \mu_T}{c} \frac{\partial^2 \bar{w}_z}{\partial y^2} + \frac{\partial \bar{v}_x}{\partial y} &= 0.
\end{aligned} \tag{31}$$

We introduce a characteristic scale of the turbulent length $\lambda_T = (\mu + \mu_T)/c$. Taking into account (27) the Equations (31) take the final form

$$\begin{aligned}
-\lambda_T \frac{\partial^2 \bar{v}_x}{\partial y^2} + \frac{\partial \bar{\varphi}_z}{\partial y} &= 0, \\
-\lambda_T \frac{\partial^2 \bar{\varphi}_z}{\partial y^2} + \frac{\partial \bar{v}_x}{\partial y} + 2\omega_z &= 0.
\end{aligned} \tag{32}$$

As the boundary conditions, we choose

$$\begin{aligned}
\bar{v}_x(h) &= v, \\
\bar{v}_x(-h) &= -v, \\
\bar{\varphi}_z(h) &= \bar{\varphi}_z(-h) = 0.
\end{aligned} \tag{33}$$

Then the solutions of equations (32) are written as

$$\bar{v}_x = \alpha v \frac{y}{h} + (1 - \alpha) v \frac{\sinh(y/\lambda_T)}{\sinh(h/\lambda_T)}, \tag{34}$$

$$\bar{w}_z = -\alpha c \frac{v}{h} t + (1 - \alpha) v \frac{\cosh(y/\lambda_T) - \cosh(h/\lambda_T)}{\sinh(h/\lambda_T)}. \tag{35}$$

In form, solutions (34) and (35) coincide with (22) and (23), but they have a different characteristic spatial scale $\lambda_T \gg \lambda$, defined by eddy viscosity. As an example, in Figure 6 we demonstrate the comparison of solution (34) with the DNS results for Couette flow with $Re = 3000$ [32] and $Re = 12800$ [33].

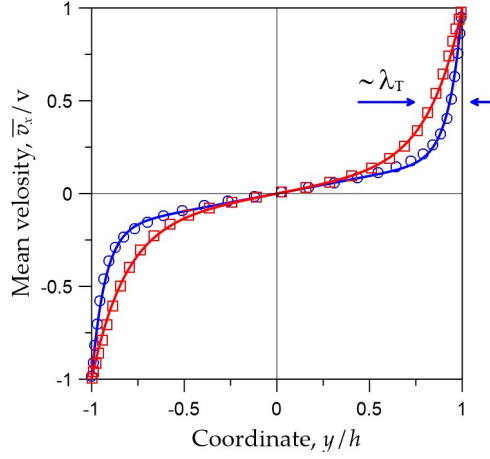


Figure 6. Distributions of the mean-velocity in a turbulent Couette flow between two moving plates. Squares (\square) are the results of DNS with $Re = 3000$ [32]; solid red line corresponds to (34) at $\lambda_T/h = 0.18$, $\alpha = 0.165$. Circles (\circ) are the DNS results with $Re = 12800$ [33]; solid blue line corresponds to (34) at $\lambda_T/h = 0.072$, $\alpha = 0.189$. The characteristic scale of the velocity profiles is $y \sim \lambda_T$.

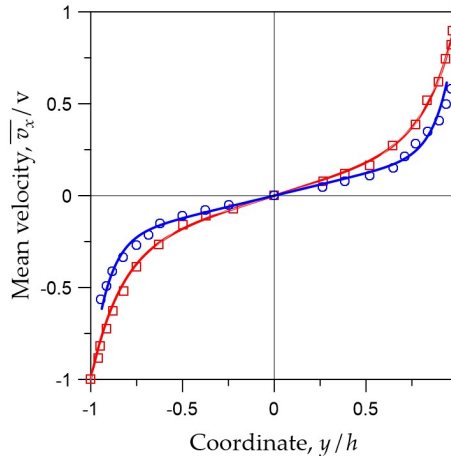


Figure 7. Distributions of the mean-velocity in a turbulent Couette flow. Squares (\square) are the experimental results for $Re = 2900$ [34]; solid red line corresponds to (34) at $\lambda_T/h = 0.16$, $\alpha = 0.3$. Circles (\circ) are the experimental results for $Re = 18000$ [34]; solid blue line corresponds to (34) at $\lambda_T/h = 0.09$, $\alpha = 0.24$.

In Fig. 7 we show the comparison of mean velocity distribution (34) with experimental results for $Re = 2900$ and 18000 [34]. It can be seen that the coincidence with experiment and DNS data is very good. We believe that it is possible to reproduce the mean velocity profile for the Couette flow with any Reynolds number by choosing corresponding combinations of the parameters λ_T and α .

8. Conclusion

Thus, we considered various types of steady state flow in the channel between two plates moving relative to each other, based on the equations describing the vortex motion of viscous fluid. We obtained several solutions corresponding to different stationary flows. As can be seen from the solution (9)-(10), the laminar motion without vortex tubes rotation is realized only in a narrow region near the plates. This regime can be important in tribology at low Re , in case of supersmooth plates sliding relative to each other, when a narrow gap between them is filled with a viscous lubricant. However, in the case of plates with rough surface, the microvortices are formed in the near-wall regions, which change the flow regime [35, 36]. The linear distribution of velocity is obtained in case when the vortex tubes rotate in-phase with the same angular velocity. On the other hand, taking into account the non-uniform phases of the tubes rotation, we obtained the interesting solutions (22)-(24), which describe the combination of previous two flows.

The proposed model of a vortex fluid allowed us to describe the stationary profile of the mean velocity in turbulent Couette flow. For this purpose, we used the Boussinesq approximation for the Reynolds shear stress tensor. In this simple case, we have obtained a closed system of equations for the time-averaged values of \bar{v}_x and \bar{w}_z , which correctly describes turbulent flow. In particular, we have shown that by optimizing the parameters $\lambda\tau$ and α in (34), it is possible to describe both experimental and DNS produced profiles of mean velocity for turbulent Couette flows with different Reynolds numbers.

References

1. T. Kambe, A new formulation of equation of compressible fluids by analogy with Maxwell's equations, *Fluid Dynamics Research*, **42**, 055502 (2010).
2. R. J. Thompson, T. M. Moeller, Numerical and closed-form solutions for the Maxwell equations of incompressible flow, *Physics of Fluids*, **30**, 083606 (2018).
3. C. R. Mendes, F. I. Takakura, E. M. C. Abreu, J. A. Neto, P. P. Silva, J. V. Frossad, Helicity and vortex generation, *Annals of Physics*, **398**, 146-158 (2018).
4. H. Marmanis, Analogy between the Navier-Stokes equations and Maxwell's equations: Application to turbulence, *Physics of Fluids*, **10**, 1428-1437 (1998).
5. S. Demir, M. Tanişli, Spacetime algebra for the reformulation of fluid field equations, *International Journal of Geometric Methods in Modern Physics*, **14**, 1750075 (2017).
6. M. Tanişli, S. Demir, N. Sahin, Octonic formulations of Maxwell type fluid equations, *Journal of Mathematical Physics*, **56**, 091701 (2015).
7. R. J. Thompson, T. M. Moeller, A Maxwell formulation for the equations of a plasma, *Physics of Plasmas*, **19**, 010702 (2012).
8. R. J. Thompson, T. M. Moeller, Classical field isomorphisms in two-fluid plasmas, *Physics of Plasmas*, **19**, 082116 (2012).
9. S. Demir, M. Tanişli, N. Sahin, M. E. Kansu, Biquaternionic reformulation of multifluid plasma equations, *Chinese journal of physics*, **55**(4), 1329 (2017).
10. C. Chanyal, M. Pathak, Quaternionic approach to dual Magneto-hydrodynamics of dyonic cold plasma, *Advances in High Energy Physics*, **13**, 7843730 (2018).
11. H. Helmholtz, "Über Integrale der hydrodynamischen Gleichungen, welche den Wirbelbewegungen entsprechen", *Journal für die Reine und Angewandte Mathematik*, **55**, 25–55 (1858). Translation. P. G. Tait, "On integrals of the hydrodynamical equations, which express vortex-motion", *Philosophical Magazine*, **33**(4), 485-512 (1867).
12. V. L. Mironov, S. V. Mironov, Generalized sedeonic equations of hydrodynamics, *European Physical Journal Plus*, **135**(9), 708 (2020).
13. V. L. Mironov, Self-consistent hydrodynamic two-fluid model of vortex plasma, *Physics of Fluids*, **33**(3), 037116 (2021).
14. V.L. Mironov, Self-consistent hydrodynamic model of electron vortex fluid in solids, *Fluids*, **7**, 330 (2022).
15. N.K. Kochin, I.A. Kibel, N.V. Roze, *Theoretical Hydrodynamics*, John Wiley & Sons, New York, 1964.
16. G.K. Batchelor, *An Introduction to Fluid Dynamics*, Cambridge University Press, 1970.
17. N. Tillmark, P.H. Alfredsson, Experiments on transition in plane Couette flow, *Journal of Fluid Mechanics*, **235**, 89-102 (1992).
18. K.H. Bech, N. Tillmark, P.H. Alfredsson, H.I. Andersson, An investigation of turbulent plane Couette flow at low Reynolds numbers, *Journal of Fluid Mechanics*, **286**, 291-325 (1995).
19. E.M. Aydin, H.J. Leuthersser, Plane-Couette flow between smooth and rough walls, *Experiments in Fluids*, **11**, 302-312 (1991).
20. S. Bottin, H. Chate, Statistical analysis of the transition to turbulence in plane Couette flow, *The European Physical Journal B*, **6**, 143-155 (1998).
21. O. Kitoh, K. Nakabyashi, F. Nishimura, Experimental study on mean velocity and turbulence characteristics of plane Couette flow: low-Reynolds-number effects and large longitudinal vortical structure, *Journal of Fluid Mechanics*, **539**, 199–227 (2005).
22. W.D. McComb, Theory of turbulence, *Reports on Progress in Physics*, **58**, 1117-1206 (1995).
23. F.S. Henry A.J. Reynolds, Analytical solution of two gradient-diffusion models applied to turbulent Couette flow, *ASME Journal of Fluids Engineering*, **106**, 211-216 (1984).
24. H.I. Andersson, B.A. Pettersson, Modeling plane turbulent Couette flow, *International Journal of Heat and Fluid Flow*, **15**(6), 447-455 (1994).

25. H. Abe, H. Kawamura, Y. Matsuo, Direct numerical simulation of a fully developed turbulent channel flow with respect to the Reynolds number dependence, *ASME Journal of Fluids Engineering*, **123**, 382-393 (2001).
26. S. Pirozzoli, M. Bernardini, P. Orlandi, Turbulence statistics in Couette flow at high Reynolds number. *Journal of Fluid Mechanics*, **758**, 327–343 (2014).
27. T. Tsukahara, H. Kawamura, K. Shingai, DNS of turbulent Couette flow with emphasis on the large-scale structure in the core region, *Journal of Turbulence*, **7**(19), 2006.
28. A. Sherikar, P.J. Disimile, Parametric study of turbulent Couette flow over wavy surfaces using RANS simulation: Effects of aspect-ratio, wave-slope and Reynolds number, *Fluids*, **5**, 138 (2020).
29. O. Reynolds, On the dynamical theory of incompressible viscous fluids and the determination of the criterion, *Philosophical Transactions of the Royal Society of London, A* **186**, 123–164 (1895).
30. J. Boussinesq, Essai sur la théorie des eaux courantes, *Mémoires présentés par divers savants à l'Académie des Sciences*, **23**(1), 1-680 (1877).
31. F.G. Schmitt, About Boussinesq's turbulent viscosity hypothesis: historical remarks and a direct evaluation of its validity, *Comptes Rendus Mécanique*, **335**(9-10), 617-627 (2007).
32. T. Tsukahara, H. Kawamura, K. Shingai, DNS Database of Wall Turbulence and Heat Transfer, Cou3000_A.dat, (<https://www.rs.tus.ac.jp/t2lab/db/>).
33. H. Kawamura, K. Shingai, Y. Matsuo, DNS Database of Wall Turbulence and Heat Transfer, Cou12800_A.dat, (<https://www.rs.tus.ac.jp/t2lab/db/>).
34. H. Reichardt, Über die Geschwindigkeitsverteilung in einer geradigen turbulenten Couetteströmung, *Zeitschrift für Angewandte Mathematik und Mechanik*, **36**, Sonderheft, 26-29 (1956).
35. M. Stanislas, L. Perret, J. M. Foucaut, Vortical structures in the turbulent boundary layer: a possible route to a universal representation, *Journal of Fluid Mechanics*, **602**, 327–382 (2008).
36. C. Wang, Q. Gao, J. Wang, B. Wang, C. Pan, Experimental study on dominant vortex structures in near-wall region of turbulent boundary layer based on tomographic particle image velocimetry, *Journal of Fluid Mechanics*, **874**, 426–454 (2019).